

# Integrated in-process chatter monitoring and automatic suppression with adaptive pitch control in parallel turning

Shuntaro Yamato<sup>1</sup> · Yuki Yamada<sup>1</sup> · Kenichi Nakanishi<sup>2</sup> · Norikazu Suzuki<sup>3</sup> · Hayato Yoshioka<sup>4</sup> · Yasuhiro Kakinuma<sup>1</sup>

Received: 4 October 2017 / Accepted: 21 April 2018 / Published online: 18 May 2018  
© Shanghai University and Springer-Verlag GmbH Germany, part of Springer Nature 2018

**Abstract** Simultaneous processes such as parallel turning or milling offer great opportunities for more efficient manufacturing because of their higher material removal rates. To maximize their advantages, chatter suppression technologies for simultaneous processes must be developed. In this study, we constructed an automatic chatter suppression system with optimal pitch control for shared-surface parallel turning with rigid tools and a flexible workpiece, integrating in-process chatter monitoring based on the cutting force estimation. The pitch angle between two tools is tuned adaptively in a position control system in accordance with the chatter frequency at a certain spindle speed, in a similar manner as the design methodology for variable-pitch cutters. The cutting force is estimated without using an additional external sensor by employing a multi-encoder-based disturbance observer. In addition, the chatter frequency is measured during the process by performing a low-computational-load spectrum analysis at a certain frequency range, which makes it possible to calculate the power spectrum density in the control system of the machine tool. Thus, the constructed system for

automatic chatter suppression does not require any additional equipment.

**Keywords** Chatter · Multitasking machine tool · Parallel turning · Adaptive control · Sensorless · Disturbance observer

## 1 Introduction

In machining, chatter is still regarded as one of the most critical issues by practicing engineers. Recently, chatter began to pose more serious problems in conjunction with trends such as increasing material removal rates (MMRs), low-friction guiding systems, and manufacturing flexible parts [1].

In order to select a stable cutting condition free from chatter, the stability lobe diagram (SLD) is widely used in conventional machining processes [2, 3]. Recently, advanced models for simultaneous machining processes, such as parallel turning [4–6] and parallel milling [7], were developed because they offered the possibility of a higher MMR and attracted increasing attention as important techniques for future multitasking machine tools. Budak and Ozturk [4] proposed a stability model for same-surface parallel turning, taking into account the dynamics of the feed direction. They revealed that dynamic interaction between tools could enhance stability compared with single-tool turning if an appropriate cutting depth was selected relative to that of another tool. Brecher et al. [5] developed dynamic model coupling through machine structure and waviness on a shared cutting surface. The dead time between two successive cuts, influenced by the radial angle between tools, affects the stability limits through dynamic coupling. In addition, Reith et al. [6] constructed a

---

✉ Shuntaro Yamato  
yamato@ams.sd.keio.ac.jp

<sup>1</sup> Department of System Design Engineering, Keio University, 3-14-1 Hiyoshi, Kohoku-ku, Yokohama 223-8522, Japan

<sup>2</sup> Nakamura-Tome Precision Industry Co., Ltd., 15 Netsuno, Hakusan, Ishikawa 920-2195, Japan

<sup>3</sup> Department of Mechanical Science and Engineering, Nagoya University, Furo-cho, Chikusa-ku, Nagoya 464-8603, Japan

<sup>4</sup> Precision and Intelligent Laboratory, Tokyo Institute of Technology, 4259-G2-19 Nagatsuta, Midori-ku, Yokohama 226-8503, Japan

mechanical model for shared-surface parallel turning to investigate the behavior of the robust stability limit in accordance with the ratio of natural frequencies between two tools. They revealed that a robustly stable chip width could be expanded by properly detuning the tools to set an optimal frequency ratio.

These developed methods reflect the trends of experimental results, and can help us understand the chatter mechanism in parallel turning. However, the accuracy of the resultant predictions is not yet sufficient to find accurate and practical chatter-free conditions because of the complicated dynamic interaction between the tools and the identification error of the tool-system dynamics and cutting coefficients, which varies depending on the tool position [8] or spindle rotations [9, 10]. Furthermore, all developed models in Refs. [4–6] postulate flexible tools in the feed direction and a much more rigid workpiece in order to avoid considering the workpiece dynamics in the radial direction. In case of a flexible workpiece, the developed stability models may be unavailable since chatter is the relative vibration between the tool and the workpiece, whose dynamics play a decisive role in chatter [11]. This is the next concern of the SLD approach in parallel turning. From the above viewpoints, along with preprocessing approaches based on the SLD, in-process chatter mitigation strategies based on chatter monitoring and feedback control in parallel turning are strongly desired for dual safety operations.

With regard to conventional processes, chatter suppression techniques have been discussed in many studies. The regenerative effect can be canceled out or attenuated with special tools such as variable pitch tools [12–14], variable helix tools [15], and serrated tools [16]. In particular, the variable pitch tool is the most practical because its optimal design methods with a comparatively simple model have been established, and it is applicable to the finishing process. Altıntaş et al. [12] extended the analytical stability model for variable pitch milling based on zero-order approximation (ZOA) in the frequency domain. On the assumptions of ZOA, Budak [13] developed an optimal design methodology for the pitch angles of an arbitrary number of flutes. The regenerative effect can be suppressed under even teeth when the phase shift between the inner and outer modulation, corresponding to the difference in pitch angles in a pair of teeth, approaches  $\pi$ . However, the optimal pitch angle is sensitive to variations in chatter frequency.

Suzuki et al. [14] introduced the regenerative factor and proposed a novel robust design method to suppress  $h$  number of vibrations mode by use of  $2^h$ -flute variable pitch cutters (VPCs). Although using variable pitch tools is an effective approach in suppressing chatter, the spindle speed and chatter frequency should be known in advance in

order to design the optimal pitch angle. Furthermore, the tool has to be redesigned if the spindle speed or chatter frequency changes significantly because the optimal pitch angle is generally sensitive to variations in chatter frequency. These are the major drawbacks for practical use of variable pitch tools in industry, especially in recent manufacturing processes such as the small-lot production of many products. More flexible techniques such as spindle speed regulation [17] and modulation [18] strategies are often used to suppress chatter. These are known as spindle speed variation (SSV) techniques. These methods offer easy implementation and flexible adjustment of SSV parameters. This is why SSV techniques are often employed for automatic chatter suppression systems combined with in-process chatter detection or monitoring. On the other hand, the SSV techniques cannot maintain an optimum phase shift to eliminate the regenerative effect. Rather, SSV techniques only reduce the effect by disrupting the phase shift owing to the spindle speed variation. Thus, the chatter suppression performance of variable pitch tools may be superior to that of SSV techniques if the optimum pitch angle is designed.

Recently, Sakata et al. [19] suppressed flexible-workpiece chatter with some robustness in shared-surface parallel turning by setting a small radial angle between tools (i.e., the pitch angle) to an optimal value. Because it is feasible to provide an angle offset to one tool in the circumferential direction with the control system of the turret position, the pitch angle can be flexibly changed as in SSV techniques. In addition, the optimal pitch angle can be determined from the chatter frequency at a certain spindle speed based on the design methodology for VPCs when chatter comes from the workpiece side. In past research [19], however, the chatter frequency was measured in advance by a preliminary cutting test under the same conditions as the main cutting, which incurred time and production costs. Furthermore, the chatter frequency that comes from a flexible workpiece will change during the process by the variation of the workpiece rigidity owing to material removal or a change in the cutting point. This necessitates adjusting the shifted pitch angle. Thus, in-process chatter measurement without preliminary cutting tests and automatic tuning of the shifted pitch angle are preferable in terms of practical applications with high flexibility and robustness.

In this study, we construct an automatic chatter suppression system with optimal pitch control for shared-surface parallel turning, integrating in-process chatter monitoring. The workpiece chatter is suppressed by real-time optimization of the pitch angle difference between tools applying a design methodology for VPCs. The chatter vibration was captured through the cutting force estimated by a multi-encoder-based disturbance observer (MEDOB)

[20], whose performance on the same multitasking machine tool was discussed in a previous study [21]. For in-process technology, the chatter frequency is identified by spectrum analysis of the estimated cutting force during the process. From the viewpoint of the computational load, the moving Fourier transform (MFT) algorithm [22] is employed in the chatter frequency range, which makes it possible to calculate the power spectrum density in the controller of the machine tool. Thus, the pitch angle in parallel turning is tuned adaptively to suppress chatter in accordance with the chatter frequency measured during the process without any additional equipment. The validity is confirmed in a small range of the pitch angle variation under a flexible-workpiece/rigid-tools assumption.

## 2 Prototype multitasking machine tool

Recently, the number of full-closed controlled ball-screw-driven machine tools equipped with linear encoders has been increasing for high-end machine tools. Figure 1a shows a prototype multitasking machine tool (Super NTY3 from Nakamura-Tome Precision Industry Co., Ltd.) that has three turrets and two work spindles. The cutting tools for parallel turning are attached to turrets 1 and 2, and each turret can move in three translational directions ( $x$ ,  $y$ , and  $z$ -axes). Figure 1b shows the machine structure and control system configuration. An optimal linear encoder (LC415, accuracy grade  $\pm 3 \mu\text{m}$ , from Heidenhain) is attached to the  $x_1$  and  $y_1$  stages. For real-time chatter monitoring and automatic suppression with unequal pitch tuning, an observer was implemented in the control system of the machine tool, which was described in detail in Sect. 3. Control signals were generated by the motion controller (Power PMAC, from Delta Tau), as shown in Fig. 1b. The

sampling frequency of the control system was 9 000 Hz (i.e., 111  $\mu\text{s}$ ). In this study, the  $y_1$  axis was employed for chatter monitoring. The major specifications of the  $y_1$  axis are listed in Table 1, and 37.5<sup>a</sup> is equivalent value of rotary-encoder resolution in translational motion considering lead length of the screw.

## 3 Methodology

### 3.1 Chatter suppression technique by unequal pitch turning

In variable pitch cutters, the chatter is suppressed by optimizing each pitch angle difference between the tooth  $j$  and the tooth  $k$ , defined as

$$\Delta\theta_{j,k} = \theta_j - \theta_k. \tag{1}$$

Figure 2 shows a concept of unequal pitch turning, assuming that the regenerative chatter comes from a flexible workpiece in the radial direction. Furthermore, the tools cut the same surface (i.e., the same depth of cut). The regenerative effect is eliminated by setting the shifted pitch angle (i.e.,  $\Delta\theta/2$ ) to a certain value, selected in a similar manner as the VPCs. When the shifted pitch angle is zero, this is conventional equal pitch parallel turning. For unequal pitch turning, the shifted pitch angle  $\Delta\theta/2$  is provided by the axial translation of the upper turret (i.e., turret 1 in Fig. 1) in the circumferential direction. To sum up, only tool 1 is moved by  $\Delta x_1$  and  $\Delta y'_1$  in the  $x_1y'_1$  plane, while the tool posture is not changed, as shown in Fig. 3. Thus, this method does not require special tools and has the flexibility of the SSV techniques.

To cancel out the regenerative effect, a proper pitch angle was selected based on the analytical design method

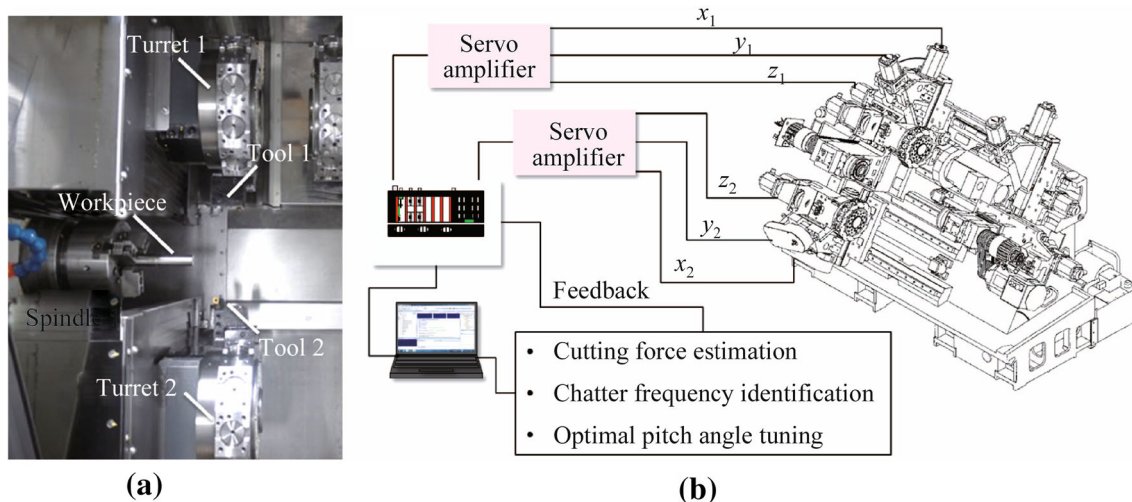
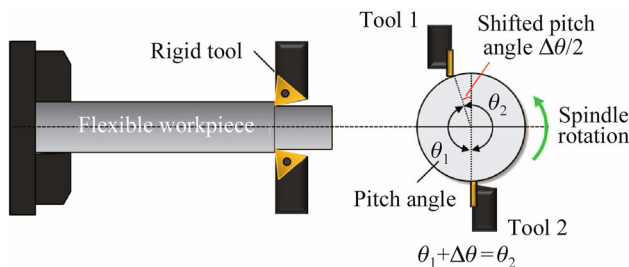


Fig. 1 Prototype of multitasking machine tool a front view and b system configuration

**Table 1** Major specifications of the prototype machine tool in  $y_1$  axis

	$y_1$
Type of guideway	Sliding
Lead length of the screw/mm	6
Drive system	Ball-screw
Reduction ratio	1
Resolution of encoders	
Linear encoder/nm	1
Rotary encoder/ $(10^3 \text{ count}\cdot\text{r}^{-1})$	160
Equivalent value/nm	37.5 <sup>a</sup>



**Fig. 2** Conceptual figure of unequal pitch turning

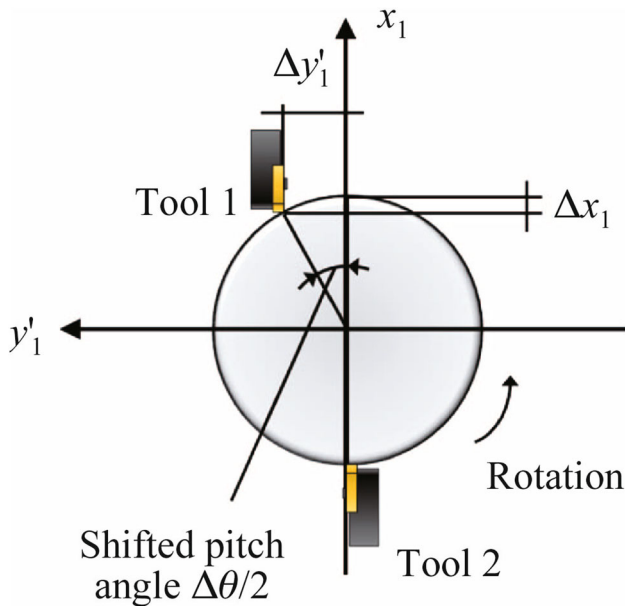


**Fig. 3** Shifted pitch angle made by turret 1 movement

for VPCs [12–14]. According to Ref. [14], the regenerative factor ( $r_f$ ), the quantitative index for the regenerative suppression effect with respect to an arbitrary chatter frequency, is defined as follows

$$r_f = \frac{1}{Z} \sum_{j=1}^Z e^{-i\varepsilon_j}, \tag{2}$$

where  $Z$  is the number of teeth, and  $\varepsilon_j(\text{rad})$  is the phase shift left on the machined surface at tooth  $j$ .  $|r_f| = 1$  in case of a regular pitch cutter. When Eq. (2) is equal to 0, the regenerative effect will disappear since paired complex phase vectors cancel out each other. In shared-surface parallel turning, the dynamic cutting area by tool 1 was influenced by the premachined surface by tool 2, and vice versa. This can be regarded as a two-flute cutter. The phase shift left on the cut surface at tool 2 is denoted as follows

$$\varepsilon_2 = \varepsilon_1 + \Delta\varepsilon, \tag{3}$$

where  $\varepsilon_1$  is the phase shift at tool 1, and  $\Delta\varepsilon$  (rad) is the difference in phase shift between the pair of teeth (i.e., tool 1 and tool 2). In alternating pitch variation (APV) or linear pitch variation (LPV) with an even number of cutters, the regenerative effect will theoretically disappear when the phase difference  $\Delta\varepsilon$  satisfies the following equation

$$\Delta\varepsilon = \varepsilon_2 - \varepsilon_1 = 2\pi \left( m + \frac{1}{2} \right), \tag{4}$$

where  $m = 0, 1, 2, \dots$ . In fact, the RF in a two-flute cutter becomes zero, as follows

$$\begin{aligned} r_f &= \frac{e^{-i\varepsilon_1} + e^{-i\varepsilon_2}}{2} \\ &= \frac{e^{-i\varepsilon_1} + e^{-i\varepsilon_1} (\cos(\pi + 2\pi m) - i \sin(\pi + 2\pi m))}{2} = 0, \end{aligned} \tag{5}$$

which means that the regenerative chatter will be suppressed. Here, the total chatter wavelength left within pitch period  $T_j$  (s) at tooth number  $j$  can be expressed as [12]

$$2\pi k_j + \varepsilon_j = 2\pi f_c T_j = \frac{60f_c}{n} \theta_j, \tag{6}$$

where  $k_j$ ,  $f_c$  (Hz),  $n$  ( $\text{min}^{-1}$ ), and  $\theta_j$  (rad) are the number of vibration marks, chatter frequency, spindle speed, and pitch angle, respectively. Thus, the total chatter wavelength existing between tool 1 and tool 2 (i.e., pitch angle  $\theta_1$ ), and between tool 2 and tool 1 (i.e., pitch angle  $\theta_2$ ) are written as follows

$$2\pi k_1 + \varepsilon_1 = \frac{60f_c}{n} \theta_1, \tag{7}$$

$$2\pi k_2 + \varepsilon_2 = \frac{60f_c}{n} \theta_2. \tag{8}$$

By subtracting Eq. (7) from Eq. (8), and substituting Eq. (4), the following equation can be derived

$$2\pi(k_2 - k_1) + 2\pi \left( m + \frac{1}{2} \right) = \frac{60f_c}{n} (\theta_2 - \theta_1). \tag{9}$$

The number of chatter marks  $k_1$  and  $k_2$  are integers that can be included in  $m$ . Therefore, the pitch angle difference  $\Delta\theta(=\theta_2 - \theta_1)$  between two tools should satisfy the following equation to cancel out the regenerative effect

$$\Delta\theta = 2\pi\left(m + \frac{1}{2}\right) \frac{n}{60f_c}. \tag{10}$$

Using Eq. (10), the optimal difference in the pitch angle between tools can be calculated from only the chatter frequency at a certain spindle speed.

However, the unequal pitch turning to suppress the chatter using Eq. (10) is valid only under the flexible-workpiece/rigid-tools assumption (i.e., the vibration comes from the workpiece). If the tools are flexible parts where the chatter occurs, the corresponding forces act on different bodies. Thus, the phase shift  $\varepsilon_j$  has no effect or is not principally responsible for the process stability [5]. In this situation, the coupled or detuned dynamics of the two tools can significantly influence the process stability, although the dynamic coupling is sensitive to the radial angle (i.e., the pitch angle) between tools [5, 6].

Furthermore, only a small pitch angle variation for unequal pitch turning is valid. Because the shifted pitch angle is applied by an axial translation of the upper turret (i.e., tool 1), the dynamic forces contributing to chatter and acting on the cutting edge are not exactly tangent and radial to the perimeter of a slender workpiece. The sum of the force vectors cannot cancel each other in unequal pitch turning. Furthermore, since the pitch angle variation is provided without tool rotation in the radial direction owing to mechanical limitations, apparent insert geometries such as the rake angle and clearance angle of tool 1 are changed. This also influences process stabilization. Thus, the difference in the phase shift  $\Delta\varepsilon$  should be kept close to  $\pi$  (i.e.,  $m = 0$ ) to prevent a large pitch variation. The optimal relation given in Eq. (10) is rewritten as Eq. (11) for unequal pitch turning.

$$\Delta\theta = \pi \frac{n}{60f_c}. \tag{11}$$

If a relatively small pitch angle variation  $\Delta\theta$  can be assumed in Eq. (11), the above influences are minimized, and these considerations may be eliminated. In the turning process, since the lobe number of the chatter is usually large, we have a good chance to obtain a small pitch angle variation.

To sum up, a flexible workpiece and small pitch angle variation are assumed for unequal pitch turning designed with the VPCs. Given these assumptions, the pitch angle difference is tuned automatically and in real time in accordance with the measured chatter frequency during the process. In the next section, a chatter monitoring method based on cutting force estimation is introduced.

### 3.2 Real-time chatter monitoring based on sensorless cutting force estimation

#### 3.2.1 Cutting force estimation by multi-encoder-based disturbance observer

In the sensorless approach, the cutting force is generally estimated using the motor current or applying the DOB theory, based on the servo information of the servomotor. However, the bandwidth for cutting force estimation is limited by structural dynamics and is not necessarily sufficient for chatter monitoring. In the full-closed controlled ball-screw-driven stage, the position response from the linear encoder is available along with the motor current and motor angle. In this case, MEDOB is applicable to the cutting force estimation. According to Ref. [21], the MEDOB-based method using the stage position from the linear encoder (i.e.,  $x_1$  and  $y_1$  axes) can monitor the vibrational state at the cutting point. On the other hand, in the DOB-based method, chatter monitoring is influenced by the damping element of the drive system, such as the guideway or belt connecting the ball screw and motor. In this study, the servo information of the  $y_1$  axis mounting the linear encoder was utilized for in-process chatter monitoring, while the  $x_1$  axis is also available.

Figure 4 shows a dual-inertia model of the ball-screw-driven stage on the  $y_1$  axis. Here, the friction force and gravity force are neglected because static components are not significant with regard to chatter frequency measurement. The variables and notations are listed in Table 2. The dynamic equations are expressed as follows

$$J_{my_1} \alpha_{my_1} = K_{ty_1} I_{ay_1, \text{ref}} - F_{\text{reacy}_1} R, \tag{12}$$

$$M_{ty_1} a_{ty_1} = F_{\text{reacy}_1} - F_{\text{cuty}_1}, \tag{13}$$

where

$$F_{\text{reacy}_1} = K_{ty_1} (R\theta_{my_1} - x_{ty_1}). \tag{14}$$

By setting up the simultaneous equations of Eqs. (12) and (13) to eliminate the reaction force term, the equation

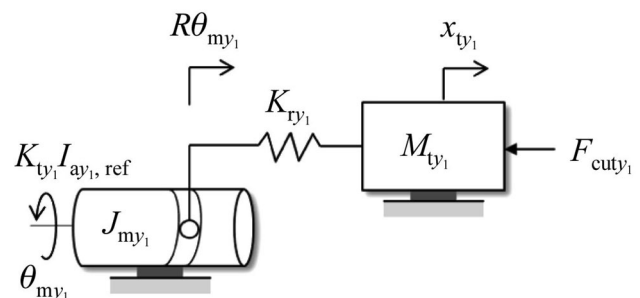


Fig. 4 Dual-inertia model of ball-screw-driven stage in  $y_1$  axis

**Table 2** Table of acronyms

Acronym	Description
$a_t/(\text{m}\cdot\text{s}^{-2})$	Acceleration of table
$F_{\text{cut}}/\text{N}$	Cutting force
$F_{\text{reac}}/\text{N}$	Reaction force
$G(s)$	Low-pass filter
$I_{a,\text{ref}}/\text{A}$	Motor current reference
$J_m/(\text{kg}\cdot\text{m}^{-2})$	Total inertia of motor, coupling and ball-screw
$K_t/(\text{N}\cdot\mu\text{m}^{-1})$	Total rigidity of feed screw system
$K_t/(\text{N}\cdot\text{m}\cdot\text{A}^{-1})$	Torque coefficient
$l/(\text{Mm})$	Lead length
$M_t/\text{kg}$	Movable mass
$R(=l/2\pi)/(\text{mm}\cdot\text{rad}^{-1})$	Transform coefficient for rotational motion to translational motion
$x_t/\text{Mm}$	Displacement of table
$\alpha_m/(\text{rad}\cdot\text{s}^{-2})$	Angular acceleration of motor
$\theta_m/\text{rad}$	Angle of motor
$(\cdot)_n$	Nominal value
$(\cdot)_{y_1}$	Value in $y_1$ direction
$\wedge$	Estimated value

for MEDOB-based cutting force estimation can be derived as

$$\hat{F}_{\text{cut}y_1} = G(s) \left( \frac{1}{R} (K_{\text{tn}y_1} I_{a y_1, \text{ref}} - J_{\text{m}n y_1} \hat{\alpha}_{\text{m}y_1}) - M_{\text{tn}y_1} \hat{a}_{\text{t}y_1} \right). \quad (15)$$

Here, a low-pass filter  $G(s)$  was implemented to eliminate high-frequency noise, whose cutoff frequency must be set higher than the expected chatter frequency range for chatter monitoring.

### 3.2.2 Methodology of spectrum analysis for in-process chatter frequency measurement

For frequency domain analysis, the fast Fourier transform (FFT), known for its low computational costs and whose calculation volume is  $O(N \log N)$ , is generally used. However, its calculation load is not low enough to perform a frequency analysis on the control system of the machine tool unless the number of analyzed data samples  $N$  is very small, which causes serious deterioration of the frequency resolution.

In chatter monitoring, entire frequency components need not be analyzed because chatter generally develops around the resonant frequency of the mechanical component. When calculating the power spectrum density at a certain frequency, the sliding discrete Fourier transform (SDFT) [23] is useful. SDFT is DFT applied to the time signal of  $N$  samples within a sliding window and recorded under sampling frequency  $F_s$  (Hz). Figure 5 shows a

schematic of SDFT. Its algorithm can be written similar to a moving average algorithm as follows

$$S_k(m) = S_k(m-1)e^{\frac{i2\pi k}{N}} + y(m) - y(m-N), \quad (16)$$

where  $S_k(m)$  is the DFT value from  $y(m-N+1)$  to  $y(m)$  at  $kF_s/N$  Hz,  $y(m)$  the analyzed signal, and  $k$  an integral number from 0 to  $N-1$ . Although the direct calculation of DFT for a single frequency component has calculation costs on the order of  $O(N)$ , that of SDFT is  $O(1)$ . Furthermore, Koike [22] extended the SDFT algorithm into a more efficient one by sacrificing the phase characteristic of the analyzed signal. This is called the MFT. The MFT algorithm is expressed as follows

$$M_k(m) \equiv S_k(m)e^{\frac{-i2\pi km}{N}} = R_k(m) + iI_k(m), \quad (17)$$

where

$$R_k(m) = R_k(m-1) - y(m-N) \cos \frac{2\pi k(m-N)}{N} + y(m) \cos \frac{2\pi km}{N}, \quad (18)$$

$$I_k(m) = I_k(m-1) - y(m-N) \sin \frac{2\pi k(m-N)}{N} + y(m) \sin \frac{2\pi km}{N}. \quad (19)$$

Although the MFT ignores the phase characteristic, the power spectrum density can be determined with fewer computations. In addition,  $k$  does not need to be an integer in the MFT algorithm. Applying MFT to multiple frequencies within the chatter vibration range, it is possible to determine the most excited frequency, which is regarded as

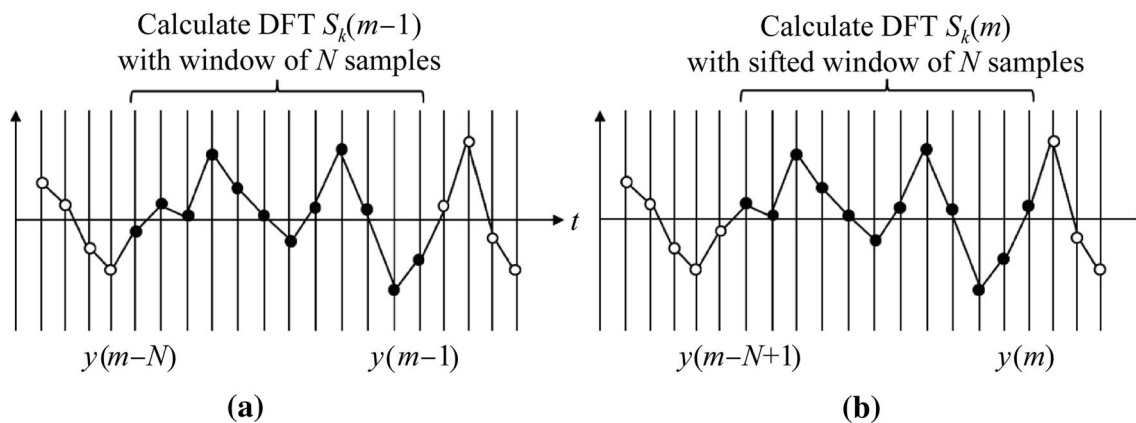


Fig. 5 Schematic of SDFT **a** before sliding, **b** after sliding

the chatter frequency in this study. The chatter range can be predicted from the frequency response functions of the mechanical component by tap testing. In this research, however, chatter is apt to occur at the workpiece side rather than the tool side because of the elongated workpiece. In this case, the frequency range where chatter is expected to occur can be roughly predicted with following equation

$$f_n = \frac{\lambda^2}{2\pi L^2} \sqrt{\frac{EI}{A\rho}}, \tag{20}$$

where  $f_n$  is the theoretical natural frequency of the bending mode for a cantilever Euler beam,  $\lambda$  a constant determined by the boundary condition and mode number,  $L$  the workpiece length, and  $A$  the section area of the cylindrical workpiece. The other variables such as  $\rho$ ,  $E$  and  $I$  are the material properties of density, Young’s modulus, and the second moment of the area, respectively. The measurement range of the chatter frequency can be limited by the predicted natural frequency.

## 4 Experimental results

### 4.1 In-process sensorless identification of the chatter frequency

To evaluate the chatter monitoring performance, conventional parallel turning (i.e., equal pitch turning) was conducted under the chatter conditions listed in Table 3. Here, the frequency range of the MFT analysis was set to 500–700 Hz with a frequency resolution of 1 Hz because the natural frequency of the first bending mode was predicted as 533 Hz by Eq. (20). The chatter frequency was measured every 4 000 servo cycles (i.e., 444 ms) by the MFT in the control system because of the calculation load limitation.

Table 3 Experimental conditions for in-process chatter identification

Variable	Value
Spindle speed/(r·min <sup>-1</sup> )	1 200
Depth of cut in each tool/mm	0.2
Feed rate/(mm·r <sup>-1</sup> )	0.15
Material of workpiece	JIS SUS303
Diameter of workpiece, $\phi$ /mm	24.9
Projection length/mm	180
Insert material	Carbide
Nose radius/mm	0.79
Rake angle/(°)	0 (neutral)
Relief angle/(°)	0
Side-edge-cutting angle/(°)	5
Analyzed frequency range in MFT/Hz	500–700
Frequency resolution of MFT/Hz	1.0
Calculation interval of MFT/Hz	2.25

Figure 6 shows the appearance of the machined workpiece and the results of the offline time-frequency analysis and online chatter frequency measurement by MFT based on the estimated cutting force in the  $y_1$  direction. The max-peak frequency (i.e., chatter frequency) was approximately captured in real time using MFT in the chatter region. Figure 7 shows the calculation error of the shifted pitch angle  $\Delta\theta/2$  relative to the measurement error of chatter frequency  $f_c$ . In Fig. 7, three cases with chatter frequencies of 560 Hz, 600 Hz, and 640 Hz at a spindle speed of 1 200 r/min were assumed. The optimal pitch calculations became more sensitive to chatter frequency measurement errors at lower chatter frequencies. The calculation error of the shifted pitch angle, however, was less than or comparable to 0.1° within  $\pm 10$  Hz measurement error of the chatter frequency. The influence of the calculation error on the shifted pitch angle, caused by the chatter frequency

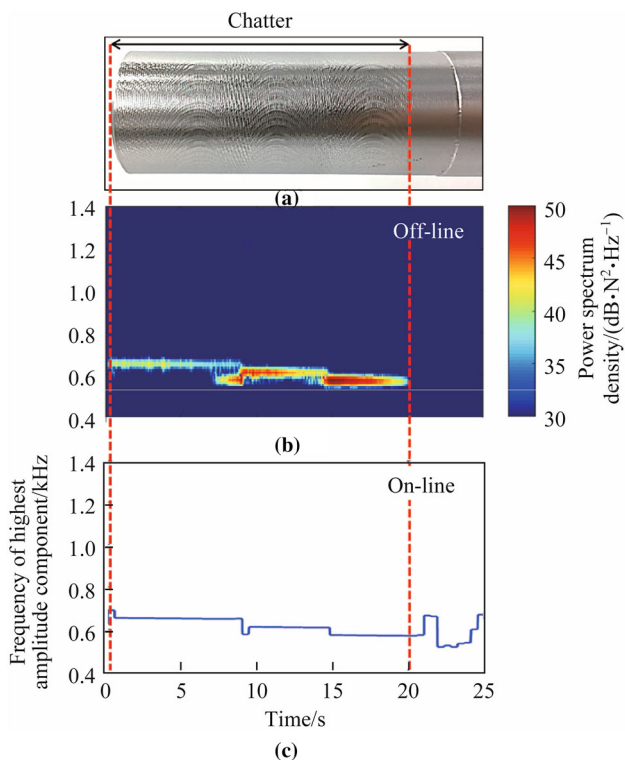


**Fig. 6** Comparison results of offline and online frequency analysis **a** machined surface, **b** time-frequency analysis result of the estimated cutting force, and **c** monitored chatter frequency by MFT

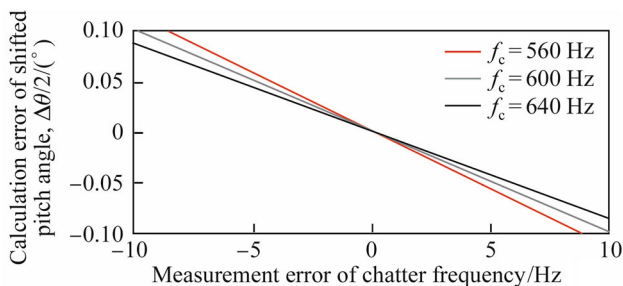


**Fig. 7** Influence of measurement error of chatter frequency on calculation error of shifted pitch angle

error, can be regarded as sufficiently small in the optimal pitch control. The performance of automatic chatter avoidance is evaluated in the next subsection.

### 4.2 Automatic chatter suppression by adaptive pitch control

Table 4 lists the experimental conditions for the outside parallel turning test. Automatic optimal pitch control with in-process chatter identification was started from the middle of the process. Here, the pitch control interval was set to 1.0 s to avoid exciting additional vibrations by translation motion of turret 1 for pitch angle variation. The pitch angle was controlled to keep the difference of phase shift

**Table 4** Experimental conditions for automatic chatter suppression by optimal pitch control (other conditions are the same as Table 3)

Variable	Value
Diameter of workpiece, $\phi$ /mm	22.1
Projection length/mm	160
Predicted resonance frequency of first bending mode/Hz	599
Analyzed frequency range in MFT/Hz	550–750
Control interval of pitch angle/s	1.0

$\Delta\epsilon$  as  $\pi$  using Eq. (11). Because the machine tool cannot change the inclination (i.e., posture) of tool 1, the apparent rake angle and clearance angle of tool 1 were changed by unequal pitch turning, which were not considered under the assumption of a small pitch angle variation.

Figure 8 shows the experimental results. As seen in Figs. 8a, b, chatter with a frequency of 738 Hz developed in the region where conventional equal pitch turning was carried out. Figure 8c presents the shifted pitch angle  $\Delta\theta/2$  and the chatter frequency estimated from MFT during the process. As soon as automatic pitch control was started at 7 s, the small pitch-angle variation was applied. The pitch angle difference was optimized in accordance with in-process chatter monitoring by MFT of the estimated cutting force on the  $y_1$  axis, and the chatter frequency component was promptly diminished. Actually, the average surface roughness  $R_a$ , measured by stylus profiling, decreased from 3.99  $\mu\text{m}$  to 1.73  $\mu\text{m}$ . Here, the shifted phase angle was perturbed just a little bit after 7 s, when no chatter existed.

Figures 9a, b show the FFT results of the estimated cutting force at 4 s (under equal pitch turning) and 15 s (under unequal pitch turning), respectively. From Fig. 9, another spectrum peak around 600 Hz, which was not observed under equal pitch turning, was excited owing to an unequal pitch, although its power spectrum density was very small. Because the frequency component that has the maximum power spectrum density calculated by MFT in the set range is simply regarded as the chatter frequency, the shifted pitch is slightly changed in accordance with the frequency around 600 Hz. To prevent unnecessary angle changes after the chatter dies out, chatter detection techniques should be used together. Since the magnitude of the power spectrum density is significantly different between the chatter and stable conditions, setting a threshold for the peak force spectrum calculated by MFT as in Ref. [18] is the simplest technique to detect chatter in this case. Furthermore, by integrating the chatter detection, the optimal pitch control can also be started automatically when chatter occurs, although the adaptive pitch control is set to start from about 7.0 s in order to compare the equal pitch and



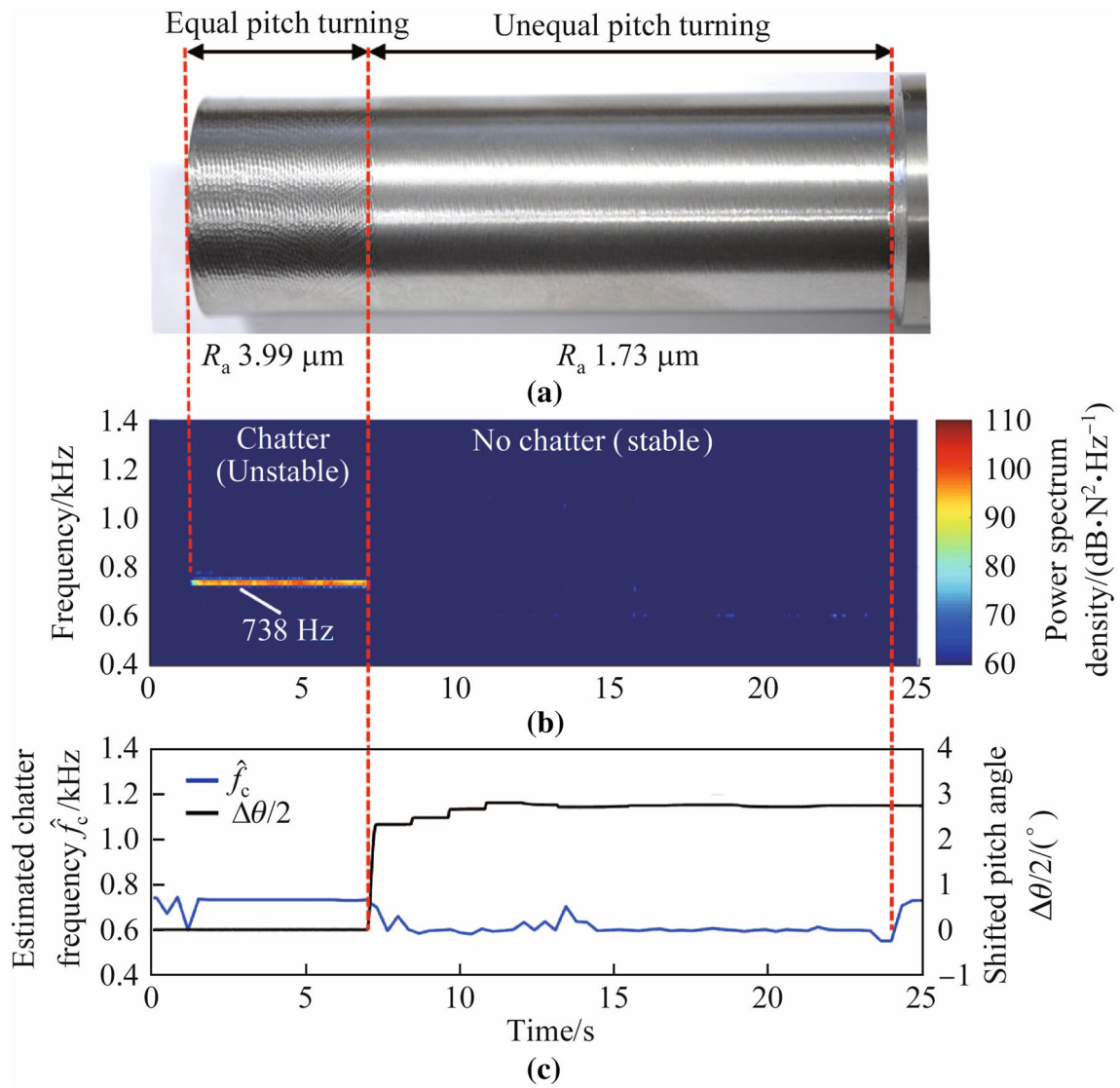


**Fig. 8** Experimental results of automatic chatter suppression by optimal pitch control **a** machined surface, **b** time-frequency analysis result of the estimated cutting force, and **c** position responses and shifted pitch angle

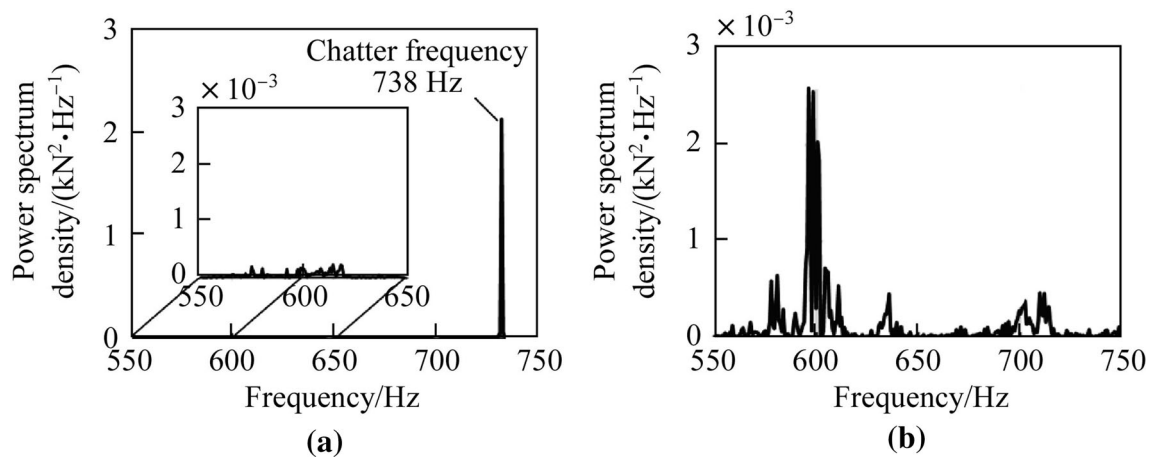


**Fig. 9** FFT results of estimated cutting force in  $y_1$  axis **a** at 4 s, **b** at 15 s

the automatic pitch control. To sum up, completely automatic active chatter suppression without any additional equipment and preliminary cutting tests will be realized.

## 5 Conclusions

In this study, an automatic chatter suppression system in accordance with the in-process measurement of chatter frequency was constructed for a flexible workpiece and shared-surface parallel turning. The pitch angle between two rigid tools can be shifted by providing an angle offset to one tool in the circumferential direction with the control system of the turret position. For workpiece-chatter suppression, the pitch angle difference was adjusted slightly during the process based on the optimal design methodology for variable pitch tools, which requires only the chatter frequency at a certain spindle speed. To capture the chatter vibration, the cutting force was estimated with only the internal information of the machine tool applying MEDOB.

From the estimated cutting force, the highest force spectrum within the chatter frequency range was identified in real time at low computational cost using MFT, which enables frequency analysis in the control system of the machine tool. Thus, all system processes (i.e., the cutting force estimation, chatter-frequency measurement, and pitch-angle shift) were completed without additional equipment or preliminary cutting tests. The system performance was verified by outside parallel turning tests under a flexible-workpiece/rigid-tool assumption. A small pitch angle variation was automatically applied setting to the optimal value based on chatter monitoring. The workpiece chatter was suppressed as soon as the pitch angle regulation started, although a small perturbation in the shifted pitch angle occurred owing to other frequency components, which can be solved by integrating chatter-detection techniques. The constructed chatter suppression system is a significant contribution to advanced intelligent machine tools with high sustainability and flexibility.

**Acknowledgements** This work was supported by the SIP Innovative Design and Production Technology Project commissioned by the New Energy and Industrial Technology Development Organization (NEDO). The authors would like to express their deepest appreciation to OMRON Corporation and Nakamura-Tome Precision Industry Co., Ltd., for their technical support to this research.

## References

- Munoa J, Beudaert X, Dombovari Z et al (2016) Chatter suppression techniques in metal cutting. *CIRP Ann Manuf Technol* 65:785–808
- Budak E, Altıntaş Y (1998) Analytical prediction of chatter stability in milling—part i: general formulation. *J Dyn Syst Meas Control* 120:22–30
- Eynian M, Altıntaş Y (2009) Chatter stability of general turning operations with process damping. *J Manuf Sci Eng* 131:41005
- Budak E, Ozturk E (2011) Dynamics and stability of parallel turning operations. *CIRP Ann Manuf Technol* 60:383–386
- Brecher C, Epple A, Neus S et al (2015) Optimal process parameters for parallel turning operations on shared cutting surfaces. *Int J Mach Tools Manuf* 95:13–19
- Reith MJ, Bachrathy D, Stepan G (2016) Optimal detuning of a parallel turning system—theory and experiments. *J Dyn Syst Meas Control* 139:14503
- Budak E, Comak A, Ozturk E (2013) Stability and high performance machining conditions in simultaneous milling. *CIRP Ann Manuf Technol* 62:403–406
- Munoa J, Beudaert X, Erkorkmaz K et al (2015) Active suppression of structural chatter vibrations using machine drives and accelerometers. *CIRP Ann Manuf Technol* 64:385–388
- Suzuki N, Kurata Y, Kato T et al (2012) Identification of transfer function by inverse analysis of self-excited chatter vibration in milling operations. *Precis Eng* 36:568–575
- Suzuki N, Nishimura K, Shamoto E et al (2010) Effect of cross transfer function on chatter stability in plunge cutting. *J Adv Mech Des Syst Manuf* 4:883–891
- Lee A, Liu CS, Chiang ST (1991) Analysis of chatter vibration in a cutter-workpiece system. *Int J Mach Tools Manuf* 31:221–234
- Altıntaş Y, Engin S, Budak E (1999) Analytical stability prediction and design of variable pitch cutters. *J Manuf Sci Eng* 121:173–178
- Budak E (2003) An analytical design method for milling cutters with nonconstant pitch to increase stability, part 1: theory. *J Manuf Sci Eng* 125:29–34
- Suzuki N, Ishiguro R, Kojima T (2016) Design of irregular pitch end mills to attain robust suppression of regenerative chatter. *CIRP Ann Manuf Technol* 65:129–132
- Yusoff AR, Sims ND (2011) Optimisation of variable helix tool geometry for regenerative chatter mitigation. *Int J Mach Tools Manuf* 51:133–141
- Koca R, Budak E (2013) Optimization of serrated end mills for reduced cutting energy and higher stability. *Procedia CIRP* 8:570–575
- Liao YS, Young YC (1996) A new on-line spindle speed regulation strategy for chatter control. *Int J Mach Tools Manuf* 36:651–660
- Altıntaş Y, Chan PK (1992) In-process detection and suppression of chatter in milling. *Int J Mach Tools Manuf* 32:329–347
- Sakata S, Kadota T, Yamada Y et al (2017) Chatter suppression in parallel turning with unequal pitch using observer based cutting force estimation. In: *Manufacturing equipment and systems*, vol 3. ASME, p V003T04A056
- Yamada Y, Kakinuma Y (2016) Sensorless cutting force estimation for full-closed controlled ball-screw-driven stage. *Int J Adv Manuf Technol* 87:3337–3348
- Yamada Y, Kadota T, Sakata S et al (2017) Integrated chatter monitoring based on sensorless cutting force/torque estimation in parallel turning. *Int J Autom Technol* 11:215–225
- Koike R (2016) Realtime monitoring and stability diagnosis of cutting process by applying disturbance observer. Dissertation. Keio University, pp 36–45
- Jacobsen E, Lyons R (2003) The sliding DFT. *IEEE Signal Process Mag* 20:74–80